PLANT MICROBIOTA

Pathogen-induced activation of disease-suppressive functions in the endophytic root microbiome

Víctor J. Carrión[1,2], Juan Perez-Jaramillo[1,3]*, Viviane Cordovez[1,2]*, Vittorio Tracanna[4]*, Mattias de Hollander[1], Daniel Ruiz-Buck[1], Lucas W. Mendes[5], Wilfred F.J. van Ijcken[6], Ruth Gomez-Exposito[1,7], Somayah S. Elsayed[2], Prarthana Mohanraju[7], Adini Arifah[7], John van der Oost[7], Joseph N. Paulson[8], Rodrigo Mendes[9], Gilles P. van Wezel[1,2], Marnix H. Medema[4]†, Jos M. Raaijmakers[1,2]†

Microorganisms living inside plants can promote plant growth and health, but their genomic and functional diversity remain largely elusive. Here, metagenomics and network inference show that fungal infection of plant roots enriched for Chitinophagaceae and Flavobacteriaceae in the root endosphere and for chitinase genes and various unknown biosynthetic gene clusters encoding the production of nonribosomal peptide synthetases (NRPSs) and polyketide synthases (PKSs). After strain-level genome reconstruction, a consortium of *Chitinophaga* and *Flavobacterium* was designed that consistently suppressed fungal root disease. Site-directed mutagenesis then revealed that a previously unidentified NRPS-PKS gene cluster from *Flavobacterium* was essential for disease suppression by the endophytic consortium. Our results highlight that endophytic root microbiomes harbor a wealth of as yet unknown functional traits that, in concert, can protect the plant inside out.

Past and present plant microbiome studies have generated a large amount of sequence data and a wealth of (mostly) descriptive information on the diversity and relative abundance of different taxonomic groups in the rhizosphere, phyllosphere, spermosphere, and endosphere of a multitude of plant species (*1*, *2*). To date, however, relatively few studies have demonstrated the functional importance of microbiomes for specific plant phenotypes, that is, plant growth, development, and health (*3*–*9*). Furthermore, the molecular and chemical basis of the causal relationships between these plant phenotypes and microbiome structure and functions are, in most cases, still unknown. The aim of this study was to investigate the genomic diversity and functional potential of the endophytic root microbiome in the protection of plants against fungal infections. To this end, we integrated multiple approaches, including network inference and metagenomics, to identify root endophytic bacterial consortia and functional gene clusters associated with a soil that is suppressive to disease caused by *Rhizoctonia solani*, a fungal root pathogen of several plant species, including rice, wheat, and sugar beet.

Disease-suppressive soils are exceptional ecosystems in which plants are protected from root pathogens as a result of antagonistic activities of the root-associated microbiome. Suppressive soils have been described for various soil-borne pathogens, including fungi, bacteria, oomycetes, and nematodes (*3*, *5*, *10*–*15*). Disease suppression can be eliminated by selective heat treatment and can be transplanted to nonsuppressive (conducive) soils, analogous to fecal transplants in humans (*5*, *16*). Specific suppression of soils to fungal root pathogens, such as *R. solani*, is induced in field soils by a disease outbreak during continuous cultivation of a susceptible host plant (*17*). Once established, the suppression can dissipate if nonhost plants are grown but is regained in the presence of the host plant and the specific fungal pathogen. Therefore, the three-way interactions between the fungal pathogen, the host plant, and its root microbiome are key elements of the onset and persistence of specific disease suppression. We previously showed that in a soil suppressive to the fungal root pathogen *R. solani*, several bacterial genera inhabiting the rhizosphere of sugar beet, in particular *Paraburkholderia*, *Pseudomonas*, and *Streptomyces* (*5*, *18*, *19*), act as a first line of defense. To understand what role microorganisms that live within plant root tissues (endophytes) play in disease suppression, we conducted a metagenomic analysis of the endosphere of sugar beet seedlings grown in field soil suppressive to *R. solani* and identified the microorganisms associated with disease suppression, distinguished which biosynthetic gene clusters (BGCs) were up-regulated during infection, reconstructed synthetic endosphere consortia, and finally made site-directed mutations to test the role of specific BGCs in disease suppression.

Taxonomic diversity and network inference of the endophytic microbiome

Sugar beet plants were grown in disease-conducive (C) and disease-suppressive (S) soils inoculated (or not) with the root pathogen *R. solani* (fig. S1). Disease incidence in the pathogen-inoculated suppressive soil (S+R) was 15 to 30%, whereas disease incidence in the pathogen-inoculated conducive soil (C+R) exceeded 80% (fig. S1A), typical of our previous studies (*5*, *16*). Given the high disease incidence in C+R, there was not enough root material left for in-depth microbiome analysis of this condition. The taxonomic diversity and functional potential of the root endophytic microbiome of plants grown in the remaining three soil conditions (C, S, and S+R) was investigated after 4 weeks of plant growth. After metagenome sequencing and bioinformatic analyses (fig. S2 and tables S1 and S2), taxonomic assignment of the microbial cell fraction from the sugar beet endosphere showed that 76.1, 10.5, and 0.0065% of the sequence reads corresponded to the domains Bacteria, Eukarya, and Archaea, respectively (fig. S3, A and B). For the eukaryotic reads, constrained analysis of principal coordinates showed significant differences [permutational multivariate analysis of variance (PERMANOVA), $P < 0.05$] between the endophytic fungal community composition in C, S, and S+R (fig. S4A). This was largely due to a statistically significant increase in *Rhizoctonia*-related sequence reads in the suppressive soil inoculated with *R. solani* (S+R) (fig. S4, B and C). Most of the other sequence reads could not be reliably assigned to specific fungal taxa. Collectively, these results indicate that after inoculation into the disease-suppressive soil, *R. solani* colonized and penetrated the plant roots but caused little disease.

16*S* ribosomal RNA (rRNA) data from the metagenome sequences (fig. S2) showed that Proteobacteria and Bacteroidetes dominated the endophytic bacterial community, with 10 operational taxonomic units spanning Pseudomonadaceae (two), Xanthomonadaceae (four), Chitinophagaceae (one), Flavobacteriaceae (two), and Veillonellaceae (one) (fig. S5), all of which became enriched in the S+R condition compared with the S condition (Fig. 1A). Co-occurrence network analysis revealed increased complexity in the S+R condition (fig. S6, A to C, and table S3) compared with C and S conditions (table S3). Highly connected

[1]Department of Microbial Ecology, Netherlands Institute of Ecology (NIOO-KNAW), Droevendaalsesteeg 10, 6708 PB Wageningen, Netherlands. [2]Institute of Biology, Leiden University, Sylviusweg 72, 2333 BE Leiden, Netherlands. [3]PECET, University of Antioquia, Medellín, Antioquia 050010, Colombia. [4]Bioinformatics Group, Wageningen University, Droevendaalsesteeg 1, 6708 PB Wageningen, Netherlands. [5]Cell and Molecular Biology Laboratory, Center for Nuclear Energy in Agriculture (CENA), University of Sao Paulo (USP), Piracicaba, Brazil. [6]Erasmus MC, University Medical Center Rotterdam, Department of Cell Biology, Center for Biomics, 3025 CN Rotterdam, Netherlands. [7]Laboratory of Microbiology, Wageningen University and Research, Stippeneng 4, 6708 WE Wageningen, Netherlands. [8]Department of Biostatistics, Product Development, Genentech Inc., South San Francisco, CA 94080, USA. [9]Laboratory of Environmental Microbiology, Brazilian Agricultural Research Corporation, Embrapa Environment, Rodovia SP 340, Km 127.5, 13820-000 Jaguariúna, Brazil.
*These authors contributed equally to this work.
†Corresponding author. Email: j.raaijmakers@nioo.knaw.nl (J.M.R.); marnix.medema@wur.nl (M.H.M.)

Downloaded from http://science.sciencemag.org/ on March 12, 2020

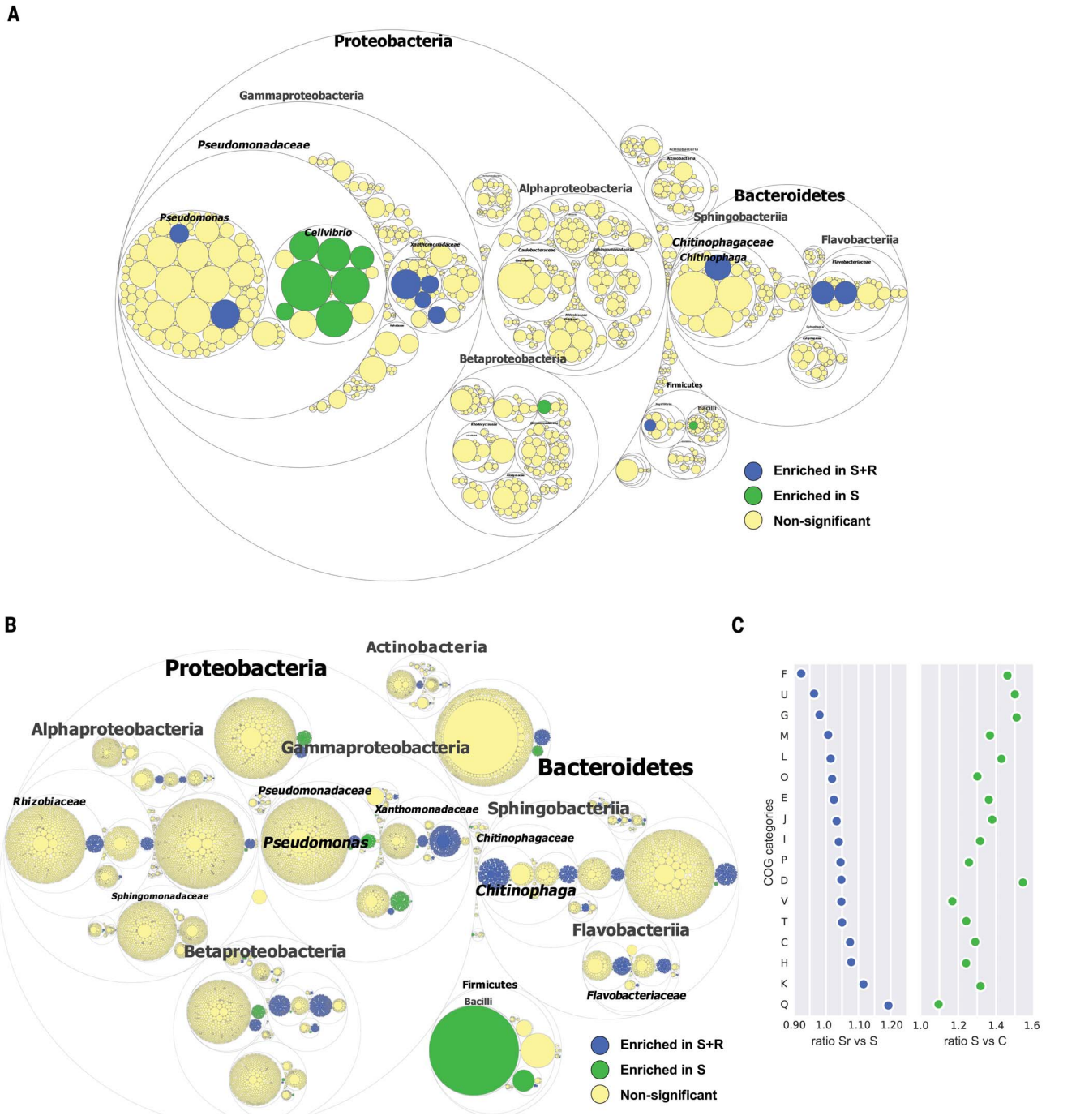


Fig. 1. Pathogen-induced changes in endophytic microbiome diversity and functions. Differential abundance of endophytic bacterial communities from plants grown in S or S+R soils. (**A**) Taxonomic differences are based on 16S rRNA sequences extracted from the metagenome. The largest circles represent phylum level, and the inner circles represent class, family, and genus. (**B**) Functional differences are based on the metagenome sequence data and assigned to taxonomic groups. The smallest circles represent the COG categories groups. The circle sizes represent the mean read relative abundance of the differentially abundant taxa and functions. Bacterial taxa or functions that are significantly enriched (FDR < 0.1) in the comparison between S and S+R are indicated in green for S and in blue for S+R; nonsignificant taxa and functions are indicated in yellow. (**C**) Strip plot depicting the average abundance ratios of all genes from Bacteroidetes belonging to core COG functional categories that contain significantly enriched genes in S+R (Sr) compared with S and in S compared with C. Categories are sorted from top to bottom by S+R/S ratio. Each COG type is abbreviated as follows: C, energy production and conversion; D, cell cycle control, cell division, and chromosome partitioning; E, amino acid transport and metabolism; F, nucleotide transport and metabolism; G, carbohydrate transport and metabolism; H, coenzyme transport and metabolism; I, lipid transport and metabolism; J, translation, ribosomal structure, and biogenesis; K, transcription; L, replication, recombination, and repair; M, cell wall, cell membrane, and cell envelope biogenesis; O, posttranslational modification, protein turnover, and chaperones; P, inorganic ion transport and metabolism; Q, secondary metabolites biosynthesis, transport, and catabolism; T, signal transduction mechanisms; U, intracellular trafficking, secretion, and vesicular transport; and V, defense mechanisms.

Downloaded from http://science.sciencemag.org/ on March 12, 2020

networks, like those in the S+R samples, can occur when microbiota face environmental perturbation, such as pathogen invasion (*20*). Interestingly, 80% of the interacting nodes in the S+R network belonged to *Chitinophaga*, *Flavobacterium*, and *Pseudomonas* species (table S4). When sequence reads from the Bacteroidetes were removed from the datasets, the endophytic signals from the C and S soils were indistinguishable (fig. S7, A and B), once again indicating an association of the Bacteroidetes genera *Chitinophaga* and *Flavobacterium* with the disease-suppressive phenotype.

Functional diversity of the endophytic microbiome

Of the genes retrieved from the metagenome data, 50 to 70% were assigned to a known function (fig. S3, C to E). For the other genes, grouping annotations indicated 56,175 taxa-associated functions, of which 402 functions were significantly enriched in the endophytic bacterial community of plants grown in the S soil compared with that of plants grown in the C soil [false discovery rate (FDR) < 0.1; fig. S8, B and C]. In the S+R condition, this proportion of functional enrichment increased more than 10-fold (4443) (FDR < 0.1; Fig. 1B). These genes belonged mainly to pathways classified as "carbohydrate transport and metabolism" and "signal transduction mechanisms." Several endophytic bacterial families—including Chitinophagaceae and Flavobacteriaceae (Bacteroidetes); Pseudomonadaceae and Xanthomonadaceae (Gammaproteobacteria); Hyphomicrobiaceae and Rhizobiaceae (Alphaproteobacteria); and Burkholderiaceae (Betaproteobacteria)—were specifically associated with the functional enrichment we observed (Fig. 1, B and C, and fig. S9A). The majority of the overrepresented genes in S+R (3138 genes of 4443) were associated with Chitinophagaceae and Flavobacteriaceae (Fig. 1B and fig. S9A). When we used a more stringent significance level of $P < 0.05$, 2063 of 56,175 taxa-associated functions were overrepresented, with 461 functions associated mainly with Chitinophagaceae and Flavobacteriaceae. Cumulative differential abundance analyses of all Bacteroidetes' genes between samples highlighted that genes from cluster of orthologous groups (COG) category Q (secondary metabolites biosynthesis, transport, and catabolism) were among the most differentially abundant between S+R and S, whereas genes from category G (carbohydrate transport and metabolism) were among the most differentially abundant between S and C (Fig. 1C).

For more detailed resolution of the specific functions associated with COGs G and Q, we searched for carbohydrate-active enzymes (CAZymes) and secondary metabolite biosynthetic gene clusters within the metagenome sequences using dbCAN (*21*, *22*) and antiSMASH (*23*), respectively. Using dbCAN, we were able to annotate 1822 genes in the endophytic metagenome with glycoside hydrolase, glycosyltransferase, polysaccharide lyase, and carbohydrate esterase domains, as well as noncatalytic carbohydrate-binding modules. Because many of these domains are evolutionary related and have related functionalities, we mapped the domain diversity in a protein family similarity network constructed using the hhsearch algorithm (*24*). Glycoside hydrolases and glycosyltransferases were more abundant in the S+R endophytic microbiome

Downloaded from http://science.sciencemag.org/ on March 12, 2020

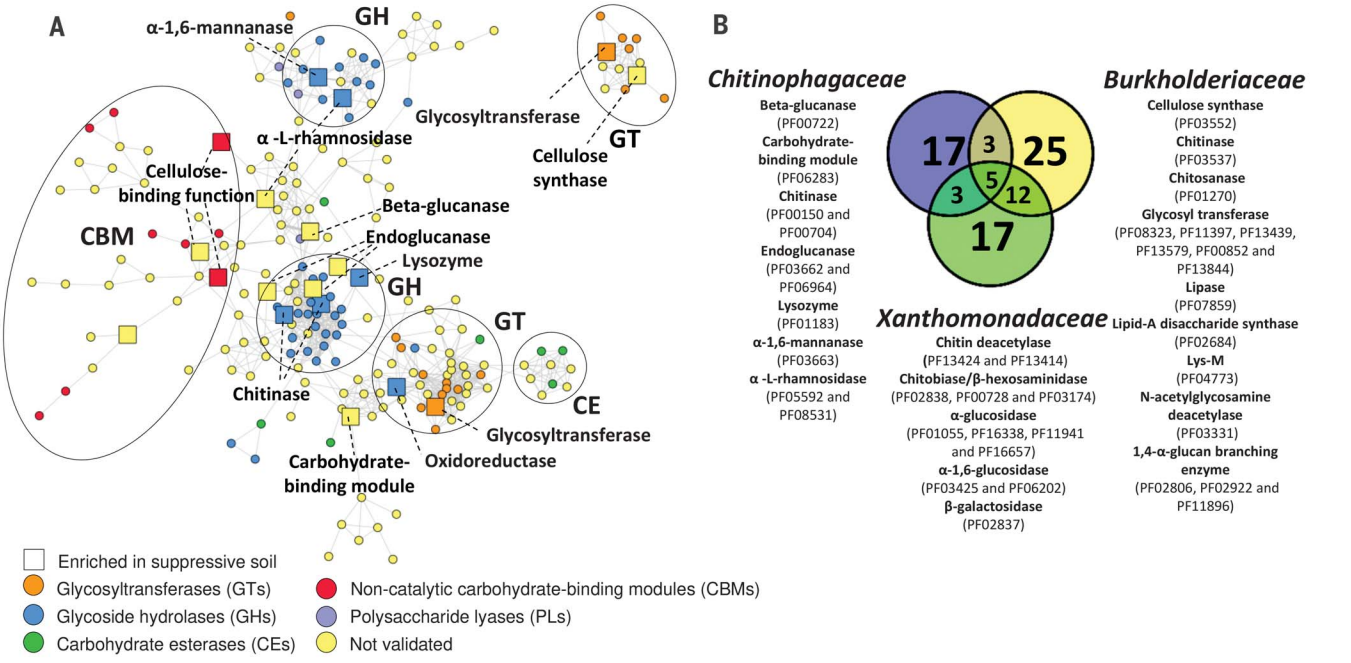


Fig. 2. Diversity and distribution of carbohydrate-active enzymes in the endophytic microbiome. (**A**) Similarity network of known and putative protein domains of enzymes involved in carbohydrate metabolism (CAZymes). From the endophytic metagenome of plants grown in suppressive soil (S) or in suppressive soil inoculated with the fungal root pathogen *R. solani* (S+R), a total of 1822 genes were annotated as CAZymes. Domain-domain distances and their relatedness are shown in the network. Nodes were grouped into five functional classes: glycoside hydrolases (GH, blue), glycosyltransferases (GT, orange), polysaccharide lyases (PL, purple), carbohydrate esterases (CE, green), and the noncatalytic carbohydrate-binding modules (CBM, red). Unknown domains or domains for which the function has not been experimentally validated are shown in yellow. Squared nodes represent enzymes that are significantly overrepresented (FDR < 0.1) in S+R compared with S and taxonomically assigned to the Chitinophagaceae. Enzymes significantly overrepresented in S+R and taxonomically classified as Burkholderiaceae and Xanthomonadaceae are shown in fig. S9, B and C, respectively. (**B**) Venn diagram with different CAZymes annotated for three endophytic bacterial families enriched in S+R, that is, Burkholderiaceae (yellow), Chitinophagaceae (blue), and Xanthomonadaceae (green). For each of the CAZymes, the Pfam number is shown in parentheses. The Venn diagram shows the number of domains detected exclusively for each bacterial family and the domains shared by these endophytic bacterial families.

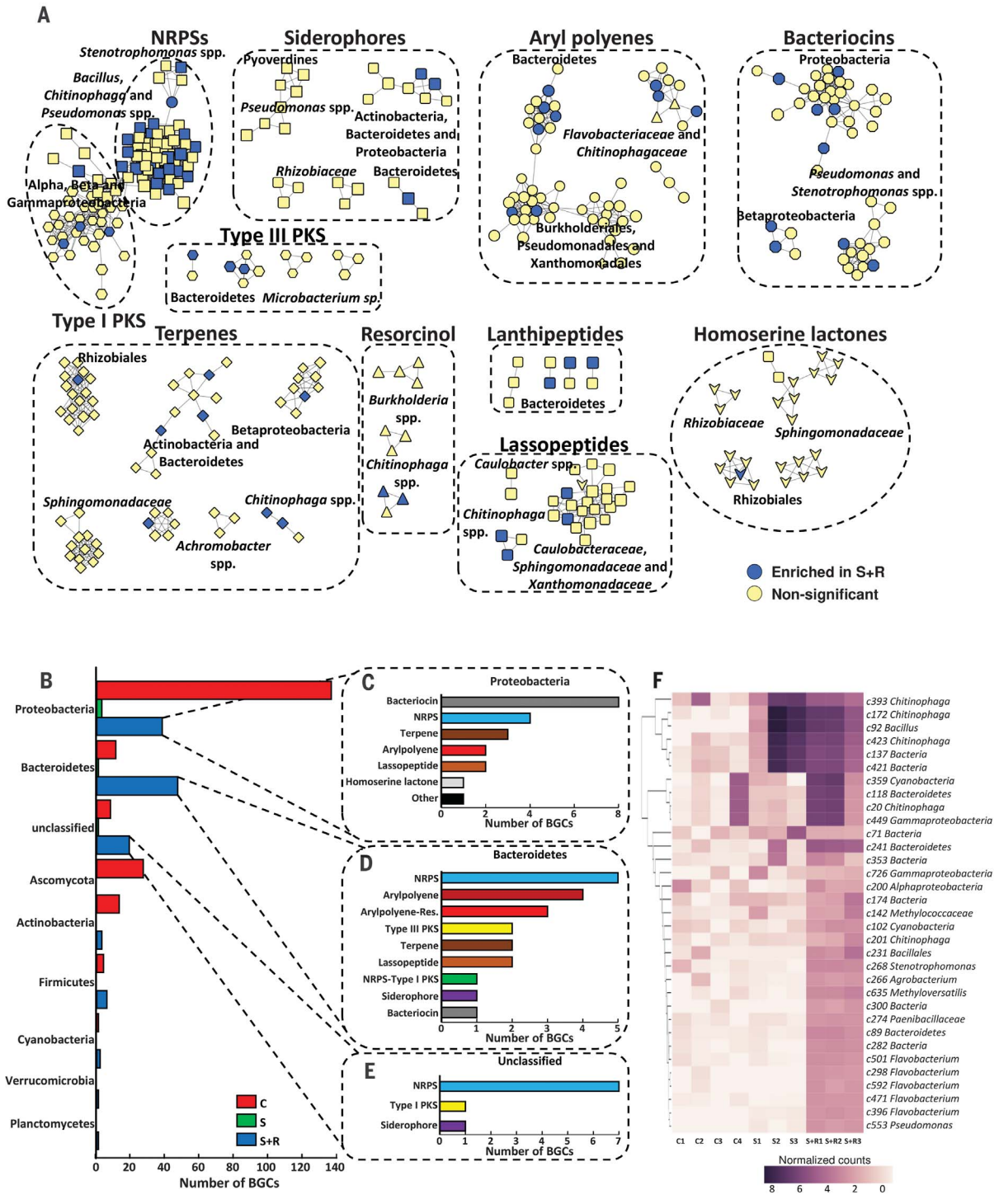


Fig. 3. Diversity and distribution of biosynthetic gene clusters in the endophytic microbiome. (**A**) Sequence similarity network [constructed with BiG-SCAPE (*32*), threshold: 0.8] of the different classes of BGCs detected in the endophytic microbiome. Taxonomic assignment and BGC class annotation of the nodes are shown. Nodes with fewer than three connections were removed; the original network with all nodes can be found in fig. S10. Node colors represent statistical significance based on a Welch's *t* test (FDR < 0.1): Yellow nodes are nonsignificant, and blue nodes are significantly overrepresented in the S+R condition. (**B**) Number of overrepresented BGCs (two-tailed Welch's *t* test, $P < 0.1$) detected by the antiSMASH and Clusterfinder algorithms for the different bacterial phyla in the endophytic root microbiome of plants grown in C, S, and S+R soils. (**C** to **E**) Number and type of BGCs assigned to Proteobacteria (C), Bacteroidetes (D), and unclassified (E) bacterial phyla that were significantly (two-tailed Welch's *t* test, $P < 0.1$) more enriched in S+R BGCs that could not be classified are not included in the (C) to (E) barplots. (**F**) Clustered heat map of relative abundances [cumulative sum scaling (CSS)–normalized RPKM (reads per kilobase per million reads) values] of the 33 NRPS gene clusters that were significantly overrepresented in the different replicate samples of S or S+R versus C. The NRPS cluster number and the corresponding taxonomic assignment are shown on the right side of the panel.

Downloaded from http://science.sciencemag.org/ on March 12, 2020

and correlated with disease suppression (Fig. 2A and fig. S9, B and C). Three endophyte families (Chitinophagaceae, Burkholderiaceae, and Xanthomonadaceae) showed statistically significant differences in CAZyme composition between S+R and S (FDR < 0.1; Fig. 2A and fig. S9, A and B). Furthermore, we found that Chitinophagaceae harbored several enzymes with domains associated with fungal cell-wall degradation, such as chitinases, β-glucanases, and endoglucanases (Fig. 2A), and also possessed debranching enzymes, including α-1,6-mannanase and α-L-rhamnosidase. Burkholderiaceae and Xanthomonadaceae families (fig. S9, B and C) also contributed two chitinase domains and three other enzymes involved in chitin degradation, including chitin deacetylase and chitosanase. Only five domains were shared between Chitinophagaceae, Burkholderiaceae, and Xanthomonadaceae (Fig. 2B), indicating limited functional redundancy among these endophytes for this trait. The enrichment of genes encoding chitin-degrading enzymes points to a role in disease suppression for these endophytes (*25*).

Bacterial genomes contain a large diversity of BGCs, the vast majority of which have not yet been linked to specific molecules or functions (*5*, *26*–*28*). Our antiSMASH analysis for secondary metabolites revealed a total of 730 BGCs associated with the biosynthesis of nonribosomal peptides, polyketides, terpenes, aryl polyenes, ribosomally synthesized and post-translationally modified peptides (RiPPs),

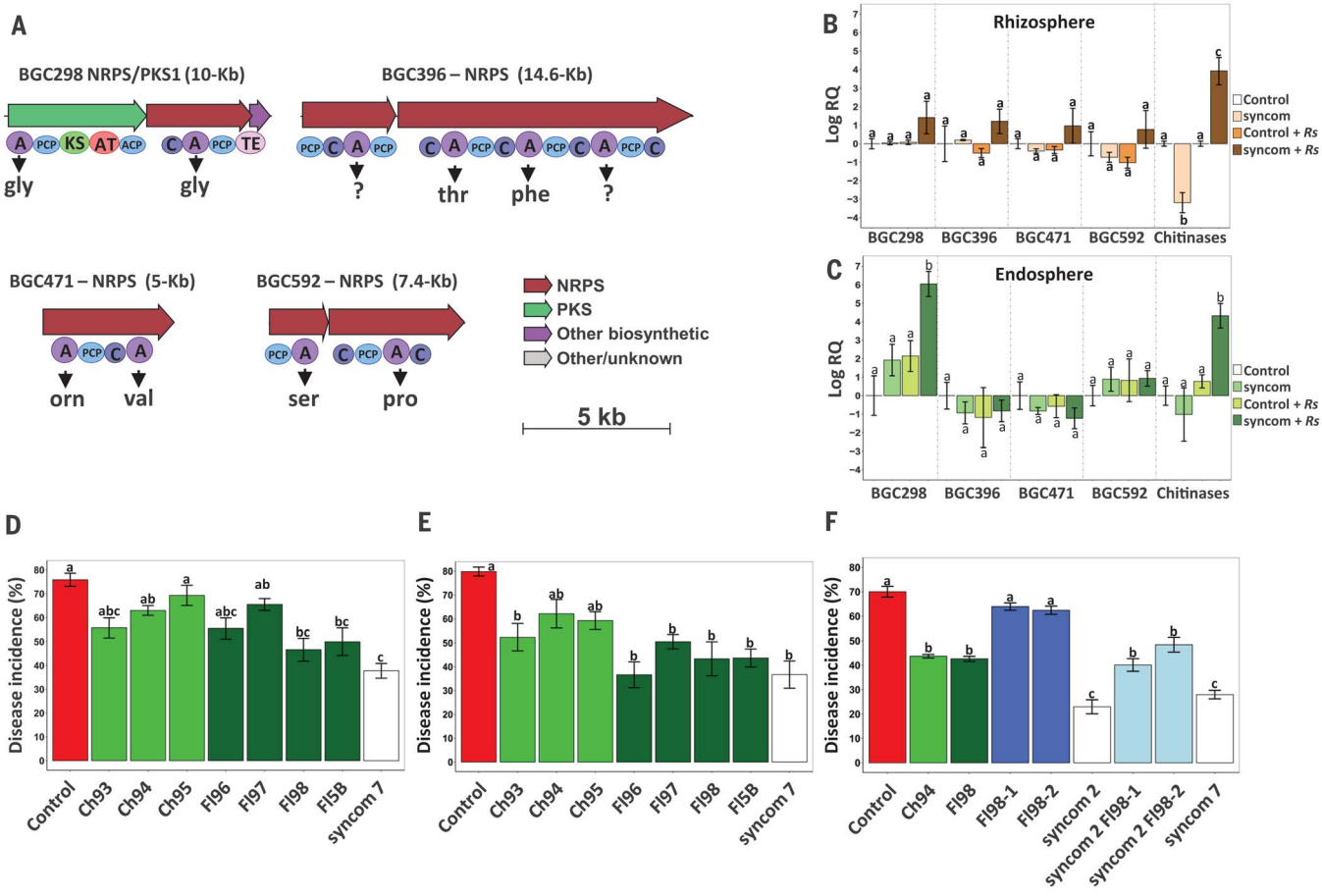


Fig. 4. Transcriptional and functional analyses of disease-suppressive consortia. (**A**) Genetic organization of BGC298, BGC396, BGC471, and BGC592 identified in both the *Flavobacterium* MAG nbed44b64 and in the genome sequences of the four endophytic *Flavobacterium* isolates. Shown below the NRPS and PKS genes are the module and domain organizations of the encoded proteins. The domains are labeled as follows: C, condensation; A, adenylation; KS, ketosynthase; AT, acyltransferase; PCP, peptide carrier protein; and TE, thioesterase. Predicted substrates of the NRPS and PKS modules in BGC298 are glycine, malonyl-CoA, and, again, glycine. (**B** and **C**) Quantitative polymerase chain reaction (qPCR)–based analysis of the expression of BGC298, BGC396, BGC471, BGC592, and chitinase genes (GH18) in the rhizosphere and endosphere of sugar beet seedlings treated with the synthetic endophytic consortium of *Chitinophaga* and *Flavobacterium* isolates (syncom). LogRQ represents the gene expression levels by relative quantification scores: Values below 0 indicate lower expression of the BGC relative to that of the housekeeping gene (*glyA*) used for data normalization. Bars represent the average of three to five biological replicates per treatment, and error bars indicate the standard error of the mean. Different letters indicate statistically significant differences between treatments as determined by one-way ANOVA with post hoc Tukey honestly significant different (HSD) test ($P < 0.05$). *Rs*, *R. solani*. (**D** to **F**) Results of three independent bioassays showing *Rhizoctonia* damping-off disease incidence of sugar beet seedlings treated with single *Chitinophaga* (Ch93, Ch94, and Ch95) and *Flavobacterium* (FI96, FI97, FI98, and FI5B) isolates and with a consortium of all seven endophytic isolates (synthetic community, syncom 7) [(D) and (E)] or treated with single *Chitinophaga* (Ch94) and *Flavobacterium* (FI98) isolates, two independent FI98 mutants (FI98-1 and FI98-2) with a deletion in BGC298, the consortium of Ch94 and FI98 (syncom 2), and syncom 7 (F). For (D) to (F), single isolates and the two syncoms were applied at an initial density of 10^7 colony forming units/g of *Rhizoctonia*-conducive field soil. Bars represent the average of four to eight biological replicates per treatment, and error bars represent the standard error of the mean. Disease incidence was scored 21 to 28 days after *R. solani* inoculation. Different letters indicate statistically significant differences between treatments as determined by one-way ANOVA with post hoc Tukey HSD test ($P < 0.05$). For (B) to (F), box plots with the individual data of each replicate are provided in figs. S20 and S21.

Downloaded from http://science.sciencemag.org/ on March 12, 2020

phosphonates, phenazines, and siderophores (Fig. 3A and figs. S10 to S12). Of these 730 BGCs, only 12 have previously been described and the chemical structure of their products elucidated (fig. S11 and table S5). Among these were the BGCs for thanamycin and brabantamide, which are two nonribosomal peptide synthetase (NRPS)–derived products previously detected in the rhizosphere microbiome of plants grown in *Rhizoctonia*-suppressive soil (*5*, *26*, *29*). For the other 718 BGCs, no near or exact matches were found for their genetic architecture and predicted products in the MIBiG repository (*27*). Of the BGCs detected, several proteobacterial RiPPs and NRPSs were noted (Fig. 3C), as well as NRPS and aryl polyene clusters originating from Bacteroidetes [mainly *Flavobacterium* and *Chitinophaga* (Fig. 3D)] and a larger proportion of NRPS clusters from contigs that could not be taxonomically assigned with confidence (Fig. 3E). Altogether, 117 BGCs were significantly overrepresented (two-tailed Welch's *t* test, $P < 0.1$) in the endosphere under the S+R conditions, with 34 BGCs belonging to Bacteroidetes (Fig. 3, A to F, and figs. S10 to S12). Notably, these did not include the thanamycin and brabantamide BGCs identified previously for the disease-suppressive *Pseudomonas* species from the rhizosphere (*5*, *29*). For the Bacteroidetes species, 10 NRPS gene clusters out of the 117 were overrepresented under S+R conditions, and none of these had a match in antiSMASH with gene clusters from MIBiG.

De novo assembly of endophytic bacterial genomes

From the 730 BGCs identified in the metagenome by antiSMASH, 157 were found in a set of 25 metagenome-assembled genomes (MAGs) that we reconstructed (figs. S13 and S14 and table S6). The MAGs, housekeeping genes, and identified BGCs were subsequently used to generate specific primer sets for transcriptome analyses and to associate the BGCs to isolates in the bacterial endophyte collection.

The initial collection of 935 bacterial endophyte isolates (fig. S1) was taxonomically characterized by 16*S* rRNA sequencing (fig. S15, A and B, and table S7), revealing eight different genera, mostly represented by Bacteroidetes and Gammaproteobacteria. Although no BGCs associated with *Chitinophaga* or *Pseudomonas* species (table S8) were detected by polymerase chain reaction (PCR) screening, four BGCs (BGC298, BGC396, BGC471, and BGC592) were found in the endophytic *Flavobacterium* isolates obtained from the S+R condition. Three of these encoded an NRPS (BGC396, BGC471, and BGC592) and the fourth a hybrid NRPS–polyketide synthase (PKS) gene cluster (BGC298, Fig. 4A). A similar approach confirmed the presence of glycosyl hydrolase (GH18) genes in three endophytic *Chitinophaga* isolates obtained from the S+R condition (Fig. 2A). Subsequent in vitro assays with the bacterial isolate collection showed that the three *Chitinophaga* isolates also had extracellular chitinolytic activity.

Subsequent genome sequencing of the three *Chitinophaga* and four *Flavobacterium* isolates showed >99% similarity among the isolates within each genus (figs. S15C and S16A and table S9). The isolate genomes also clustered with MAGs assigned to each of these genera (fig. S15, B and C), confirming that they correspond to taxa abundant in the microbiome. For the key BGCs, no signs of metagenome misassemblies were identified on the basis of comparisons with the complete genome sequences of the Bacteroidetes isolates (figs. S16, B and C, and S17, A to C).

Reconstruction and functional analysis of disease-suppressive consortia

We selected the seven sequenced Bacteroidetes isolates for root colonization assays and BGC-transcript analysis. All isolates colonized the rhizosphere and the root endosphere of sugar beet seedlings (figs. S18 and S19). Transcriptional analysis showed that chitinase expression was significantly ($P < 0.05$) higher in the consortium colonizing the rhizosphere and endosphere compartments inoculated with the fungal pathogen (Fig. 4, B and C, and fig. S20). Of the four *Flavobacterium* gene clusters, BGC298 was expressed at significantly ($P < 0.05$) higher levels in the endosphere than in the rhizosphere when the plant roots were challenged with the fungal pathogen *R. solani* (Fig. 4C). This BGC was consistently assembled in all four *Flavobacterium* genomes and in a MAG (fig. S16B) and showed no match with known BGCs in MIBiG (fig. S17).

The central place of *Flavobacterium* and *Chitinophaga* in the functional network of plants grown in the disease suppressive soil, their ability to colonize the endosphere, and the fact that expression of BGC298 and chitinase genes in the synthetic consortium are induced by the fungal pathogen suggest a role in *R. solani*-disease suppression. To test this hypothesis, three independent bioassays showed that the consortium of *Chitinophaga* and *Flavobacterium* conferred significant and more consistent protection against fungal root infection than the individual consortium members (Fig. 4, D to F, and fig. S21, A to C). Even when single isolates showed little benefit against disease, consortia always showed a greater degree of protection (Fig. 4, D to F, and fig. S21, A to C). The apparent "minimal" consortium to reconstitute the plant phenotype consisted of one *Chitinophaga* isolate and one *Flavobacterium* isolate (syncom-2), because this consortium showed the same level of disease control observed for the seven-member consortium (syncom-7; Fig. 4F).

To confirm the role of the *Flavobacterium* BGC298 in the disease-suppressive activity, we developed a SpyCas9-mediated system for introduction of double-stranded DNA breaks in *Flavobacterium* sp. 98. We obtained two independent BGC298 mutants (fig. S22, A to D, and tables S10 to S12), for which the PKS gene deletion was verified by Sanger sequencing with specific primers (fig. S22D). The two mutants colonized the rhizosphere and endosphere to the same extent as wild-type *Flavobacterium* sp. 98 when introduced alone or with *Chitinophaga* sp. 94 (table S13). When the two independent BGC298 mutants were tested in the disease bioassay, the mutation reduced disease-suppressive activity of *Flavobacterium* sp. 98 alone and when paired with the *Chitinophaga* isolate (Fig. 4F).

Conclusions

In our previous studies on soils suppressive to fungal root diseases, we showed that rhizosphere bacteria act as first line of defense (*5*–*7*, *10*). If the pathogen breaks through this first line of defense, it will encounter the basal and induced defense mechanisms of the plant (*30*). Here, we show that in this second stage of pathogen invasion of the plant roots, the endophytic microbiome can provide an additional layer of protection. Our experiments showed that on pathogen invasion, members of the Chitinophagaceae and Flavobacteriaceae became enriched within the plant endosphere and showed enhanced enzymatic activities associated with fungal cell-wall degradation, as well as secondary metabolite biosynthesis encoded by NRPSs and PKSs. After de novo assembly of 25 bacterial genomes from metagenome sequences, we were able to reconstruct a synthetic community (syncom) of *Flavobacterium* and *Chitinophaga* that provided disease protection. Site-directed mutagenesis further confirmed the contribution of BGC298 in *Flavobacterium* to this phenotype. Where these two bacterial genera are localized inside the root tissue and how they interact at the molecular level in the endosphere is not yet known. Possibly, chitinase-generated chitooligosaccharides induce expression of the *Flavobacterium* BGC298. Whether BGC298 encodes a metabolite that exerts direct antifungal activity or acts as a regulator of other protective traits is not yet known. Another consideration is that the consortium may have indirect effects through induction of local or systemic resistance in the roots. The results of this study highlight the wealth of as yet unknown microbial genera and functional traits in the endophytic root microbiome. Adopting metagenome-guided analyses and network inference was successful in pinpointing taxa and functions for targeted design of microbial consortia to attain a specific microbiome-associated plant phenotype.

Downloaded from http://science.sciencemag.org/ on March 12, 2020

REFERENCES AND NOTES

1. J. A. Vorholt, C. Vogel, C. I. Carlström, D. B. Müller, *Cell Host Microbe* **22**, 142–155 (2017).
2. V. Cordovez, F. Dini-Andreote, V. J. Carrión, J. M. Raaijmakers, *Annu. Rev. Microbiol.* **73**, 69–88 (2019).
3. M.-J. Kwak *et al*., *Nat. Biotechnol.* **36**, 1117 (2018).
4. S. Hacquard *et al*., *Cell Host Microbe* **17**, 603–616 (2015).
5. R. Mendes *et al*., *Science* **332**, 1097–1100 (2011).
6. K. Panke-Buisse, A. C. Poole, J. K. Goodrich, R. E. Ley, J. Kao-Kniffin, *ISME J.* **9**, 980–989 (2015).
7. N. Vannier, M. Agler, S. Hacquard, *PLOS Pathog.* **15**, e1007740 (2019).
8. B. O. Oyserman, M. H. Medema, J. M. Raaijmakers, *Curr. Opin. Microbiol.* **43**, 46–54 (2018).
9. P. Durán *et al*., *Cell* **175**, 973–983.e14 (2018).
10. D. M. Weller, J. M. Raaijmakers, B. B. M. Gardener, L. S. Thomashow, *Annu. Rev. Phytopathol.* **40**, 309–348 (2002).
11. E. Chapelle, R. Mendes, P. A. H. M. Bakker, J. M. Raaijmakers, *ISME J.* **10**, 265–268 (2016).
12. R. L. Berendsen, C. M. J. Pieterse, P. A. H. M. Bakker, *Trends Plant Sci.* **17**, 478–486 (2012).
13. M. Mazzola, *J. Nematol.* **39**, 213–220 (2007).
14. R. Mendes, P. Garbeva, J. M. Raaijmakers, *FEMS Microbiol. Rev.* **37**, 634–663 (2013).
15. J.-Y. Cha *et al*., *ISME J.* **10**, 119–129 (2016).
16. M. van der Voort, M. Kempenaar, M. van Driel, J. M. Raaijmakers, R. Mendes, *Ecol. Lett.* **19**, 375–382 (2016).
17. J. M. Raaijmakers, M. Mazzola, *Science* **352**, 1392–1393 (2016).
18. V. J. Carrión *et al*., *ISME J.* **12**, 2307–2321 (2018).
19. V. Cordovez *et al*., *Front. Microbiol.* **6**, 1081 (2015).
20. K. Faust, J. Raes, *Nat. Rev. Microbiol.* **10**, 538–550 (2012).
21. Y. Yin *et al*., *Nucleic Acids Res.* **40**, W445–W451 (2012).
22. V. Lombard, H. Golaconda Ramulu, E. Drula, P. M. Coutinho, B. Henrissat, *Nucleic Acids Res.* **42**, D490–D495 (2014).
23. T. Weber *et al*., *Nucleic Acids Res.* **43**, W237–W243 (2015).
24. M. Remmert, A. Biegert, A. Hauser, J. Söding, *Nat. Methods* **9**, 173–175 (2011).
25. S. M. Bowman, S. J. Free, *BioEssays* **28**, 799–808 (2006).
26. J. Watrous *et al*., *Proc. Natl. Acad. Sci. U.S.A.* **109**, E1743–E1752 (2012).
27. M. H. Medema *et al*., *Nat. Chem. Biol.* **11**, 625–631 (2015).
28. P. Cimermancic *et al*., *Cell* **158**, 412–421 (2014).
29. Y. Schmidt *et al*., *ChemBioChem* **15**, 259–266 (2014).
30. J. D. G. Jones, J. L. Dangl, *Nature* **444**, 323–329 (2006).
31. V. J. Carrión, M. de Hollander, V. Tracanna, Pathogen-induced activation of disease suppressive functions in the endophytic root microbiome. Zenodo (2019); http://doi.org/10.5281/zenodo.3405564.
32. J. Navarro-Muñoz *et al*., A computational framework for systematic exploration of biosynthetic diversity from large-scale genomic data. bioRxiv 445270 [Preprint] (17 October 2018); https://doi.org/10.1101/445270.

ACKNOWLEDGMENTS

We thank I. de Bruijn, S. P. Vega-Hernández, V. de Jager, and R. Keijzer for their valuable advice on genomic and metagenomic DNA extractions. We would also like to thank the BSc and MSc students C. Rotoni, R. Hijkoop, H. McDermott, A. Nurfikari, J. Spooren, and R. Peters for their valuable help with the *Flavobacterium* and *Chitinophaga* isolation and phenotyping. We thank M. J. McBride at the University of Wisconsin for providing the plasmids for *Flavobacterium* transformation. This is publication number 6824 of the NIOO-KNAW. **Funding:** J.M.R. and V.J.C. were supported by grants from the Netherlands BE-Basic Foundation and the Dutch TTW-Perspective program Back to the Roots. V.J.C. was also supported by a fellowship from the Junta de Andalucía (Proyecto de Excelencia, P07-AGR-02471) and Plan Propio of the University of Málaga. V.C. and S.S.E. were supported by the Dutch STW-program Back to the Roots. J.P.-J. was financially supported by the Department of Science, Technology, and Innovation of Colombia–COLCIENCIAS through doctoral grant 568-2012-15517825. **Author contributions:** V.J.C., V.C., D.R.-B., S.S.E., and J.P.-J. designed and conducted the experiments. R.G.-E. contributed to the soil sample collection. V.J.C. and W.F.J.v.I. generated the metagenome data. P.M., A.A., and J.v.d.O. made the *Flavobacterium* mutants. Data were analyzed by V.J.C., J.P.-J., V.T., L.W.M., M.H.M., J.N.P., and M.d.H. Funding acquisition and project management was provided by J.M.R. The manuscript was written by V.J.C., R.M., G.P.v.W., M.H.M., and J.M.R. All authors read and approved the final manuscript. **Competing interests:** M.H.M. is a member of the Scientific Advisory Board of Hexagon Bio and co-founder of Design Pharmaceuticals. All other authors declare that they have no competing interests. **Data and materials availability:** All data needed to evaluate the conclusions in the paper are present in the paper and/or the supplementary materials. The sequencing data are available under European Bioinformatics Institute (EBI) submission number PRJEB8920. Data, scripts, and code used for statistical and bioinformatic analyses are available at (*31*).

SUPPLEMENTARY MATERIALS

science.sciencemag.org/content/366/6465/606/suppl/DC1
Materials and Methods
Figs. S1 to S22
Tables S1 to S14
References (*33*–*95*)

View/request a protocol for this paper from *Bio-protocol*.

7 February 2019; resubmitted 21 July 2019
Accepted 17 September 2019
10.1126/science.aaw9285

Downloaded from http://science.sciencemag.org/ on March 12, 2020

Science

Pathogen-induced activation of disease-suppressive functions in the endophytic root microbiome

Víctor J. Carrión, Juan Perez-Jaramillo, Viviane Cordovez, Vittorio Tracanna, Mattias de Hollander, Daniel Ruiz-Buck, Lucas W. Mendes, Wilfred F.J. van Ijcken, Ruth Gomez-Exposito, Somayah S. Elsayed, Prarthana Mohanraju, Adini Arifah, John van der Oost, Joseph N. Paulson, Rodrigo Mendes, Gilles P. van Wezel, Marnix H. Medema and Jos M. Raaijmakers

Science **366** (6465), 606-612.
DOI: 10.1126/science.aaw9285

Protecting plants from the inside out

Some soils show a remarkable ability to suppress disease caused by plant pathogens, an ability that is attributed to plant-associated microbiota. Carrión *et al.* investigated the role of endophytes, the intimate microbial community found within roots, in fungal disease suppression (see the Perspective by Tringe). The wilt fungus *Rhizoctonia solani* infects sugar beets, whereupon transcriptional analysis shows that several bacterial endophyte species activate biosynthetic gene clusters to cause disease suppression. These organisms produce antifungal effectors, including enzymes that can digest fungal cell walls, and secondary metabolites, including phenazines, polyketides, and siderophores, which may contribute to the antifungal phenotype.

Science, this issue p. 606; see also p. 568

ARTICLE TOOLS http://science.sciencemag.org/content/366/6465/606

SUPPLEMENTARY MATERIALS http://science.sciencemag.org/content/suppl/2019/10/30/366.6465.606.DC1

RELATED CONTENT http://science.sciencemag.org/content/sci/366/6465/568.full

REFERENCES This article cites 89 articles, 14 of which you can access for free
http://science.sciencemag.org/content/366/6465/606#BIBL

PERMISSIONS http://www.sciencemag.org/help/reprints-and-permissions

Use of this article is subject to the Terms of Service

Science (print ISSN 0036-8075; online ISSN 1095-9203) is published by the American Association for the Advancement of Science, 1200 New York Avenue NW, Washington, DC 20005. The title *Science* is a registered trademark of AAAS.

Copyright © 2019 The Authors, some rights reserved; exclusive licensee American Association for the Advancement of Science. No claim to original U.S. Government Works

Downloaded from http://science.sciencemag.org/ on March 12, 2020